Journal of Integrative Neuroscience

*J. Integr. Neurosci.* **2022**; 21(6): 170
https://doi.org/10.31083/j.jin2106170

*Original Research*

# The Switching Rates of Dynamic Functional Networks Differently Contribute to Cross-Sectional and Longitudinal Cognition in Mild Cognitive Impairment

Zhen Hu[1,2], Yulei Deng[1,2,3], Binyin Li[2,3,*]

[1]Department of Neurology, Ruijin Hospital Lu Wan Branch, Shanghai Jiao Tong University School of Medicine, 200025 Shanghai, China
[2]Clinical Neuroscience Center, Ruijin Hospital Lu Wan Branch, Shanghai Jiao Tong University School of Medicine, 200025 Shanghai, China
[3]Department of Neurology and Institute of Neurology, Ruijin Hospital, Shanghai Jiao Tong University School of Medicine, 200025 Shanghai, China
*Correspondence: libinyin@126.com (Binyin Li)

Academic Editor: Giovanna Zamboni
Submitted: 6 June 2022 Revised: 20 July 2022 Accepted: 21 July 2022 Published: 28 October 2022

**Abstract**

**Background**: The relationship between switching rate of multilayer functional network and cognitive ability in mild cognitive impairment (MCI) and Alzheimers' disease remains unclear. **Methods**: We followed up MCI patients for one year and analyzed the association of switching rates with cognitive decline. The iterative and ordinal Louvain algorithm tracked the switching of functional networks, while elastic network regression and Bayesian belief networks were used to test the relationship between network switching rate and cognitive performance cross-sectionally and longitudinally. **Results**: The switching rate of the default mode network positively correlated with better cognitive function, while that of salience and executive control network was negatively associated with memory and executive function. The lower default mode network (DMN) switching rate predicted MCI progression to dementia, while the lower sensorimotor network switching rate heralded in slower cognitive decline. **Conclusions**: The present study investigated the predictive effect of switching rate on cognitive performance, as well as MCI progression to dementia. The inverse effect from different functional networks may become useful for early diagnosis and revealing the mechanism of neural networks in cognitive decline.

**Keywords:** mild cognitive impairment; Alzheimer's disease; dynamic functional network; functional MRI

## 1. Introduction

As the potential early stage of Alzheimer's disease (AD), mild cognitive impairment (MCI) was largely studied about its progression to AD. About 10–12% of MCI patients converted to AD annually, and the rate became 25–30% at three years. Overall, more than 60% of MCI patients eventually developed AD [1,2]. The judgment of MCI progression in the early stage was a crucial step to attain further medical intervention. Various predictive models have been generated, combing demographics, genetical factors, brain structure, and functional connectivity, amyloid deposition, and tauopathy [3–6]. The comprehensive analysis of multimodal information has made these models of relatively high accuracy. However, we still need to explore how the cognition related brain activity changes in this critical stage, as well as predictive effect of brain network.

During the past two decades, resting-state functional magnetic resonance imaging (rs-fMRI) has developed rapidly, which has promoted the understanding of the human brain. The neural network was regarded as the basis of human cognition. However, the traditional study of the brain network was based on the static description of brain functional connectivity (FC) from rs-fMRI. In the process of cognitive activity, the neural network reorganized dynamically [7]. Based on the analysis of temporally dynamic changes of the blood oxygen level-dependent (BOLD) signal in the resting state, it is found that the dynamic functional network connection (dFNC) modes fluctuated spontaneously.

The dynamic functional connection of the brain network was tried to predict the change of cognition, which greatly promoted the understanding of brain cognition, brain development, and the neural mechanism of brain diseases [8]. However, the dynamic FC or dFNC analysis still did not reflect real temporal changes of specific networks, as there would be a gap between BOLD signals and real neural network. Moreover, traditional clustering method, such as k-means or distribution-based clustering, did not fully make use of the dynamic temporal information.

Multilayer network analysis provided a novel method to process the complex data of multivariate and multi-scale information [9]. The multi-layer modularization algorithm introduced the time and space of networks, and the decomposed networks had a non-overlapping period and space. The multilayer modular model could quantify the dynamic FC and track the temporal changes of each network. In this way each network had a unique switching rate, which refers to the degree of network switching between different modules in the multilayer network. In other words, the multilayer modularity model and switching rate allowed us to track the temporal network of a specific one and quantify their changes [10].

Previous studies had used the switching rate as a marker to predict various cognitive performance in healthy people [7,11,12], as well as in the severity of mental and neurological diseases with cognitive impairment, such as schizophrenia and epilepsy [13,14].

It is the first time that the dynamic network switching rate from fMRI is estimated as an effective index to predict cognition in MCI. We assume that the switching rate of networks from fMRI can predict the cognitive changes of MCI and become a new functional neuroimaging biomarker for MCI progression. Given that the network serves as the basis of cognitive activity, we also tend to find critical networks accounting for cognition changes during the MCI stage.

## 2. Materials and Methods

### *2.1 Participants*

The study was observational and used data from the control group of MCI in the SIMPLE cohort (detailed information is available in [1]). The cohort recruited MCI patients with age between 50 to 80 years from memory clinics or community. After screened by neurologists, patients with cognitive decline caused by other diseases were excluded (including but not limited to cerebrovascular disease, central nervous system infections, Parkinson's disease, metabolic encephalopathy, deficiency of folic acid/vitamin B12 and hypothyroidism). The patients were diagnosed according to the National Institute on Aging-Alzheimer's Association (NIA-AA) workgroups [15]. Participants present mild cognitive problems based on the Mini-Mental State Examination and Clinical Dementia Rating scale (0.5). All MCI cases had medial temporal lobe atrophy (MTA) score above Grade II. Further, we exclude patients with MRI artifacts. The imaging and cognitive data were collected in the same day.

In total, we included 118 MCI patients (mean age, 65.39 $\pm$ 6.97; 19 male and 40 female patients). Among them, 14 patients progressed to AD after 12-month follow-up (pMCI group, mean age, 69.14 $\pm$ 5.64; 2 male and 12 female patients), while the other 104 remained stable (sMCI group, mean age, 64.88 $\pm$ 7.02; 36 male and 68 female patients).

After the baseline assessment, patients would be followed up without any intervention for cognition and had the identical neuropsychological assessment after 12 months. AD was diagnosed at the 12-month follow-up if patients met the diagnostic criteria of dementia due to AD (described in [1], according to the National Institute on Aging-Alzheimer's Association (NIA-AA) workgroups [15]). The AD criteria included decline from previous levels of functioning and significant cognitive symptoms which impaired activities of daily living. The diagnosis was made by a skilled clinician based on the individual circumstances of the patient and were further were confirmed by $^{18}$F-Florbetapir PET [16]. These patients were defined as progressed MCI (pMCI). The others were considered as stable MCI (sMCI). Each patient signed written informed consent, and Ruijin Hospital's ethical committees had approved the study.

### *2.2 Neuropsychological Assessment*

Baseline demographics include sex, age, and education level, listed in Table 1. Neuropsychological battery for multiple cognitive domains was administered to all patients, including Alzheimer's Disease Assessment Scale-Cognitive subscale (ADAS-Cog) [17], the Auditory Verbal Learning Test (AVLT) - Huashan version [18], the Trail Making Test (TMT, including Part A and B) [19], the Rey-Osterrieth Complex Figure Test (CFT) [20], the Stroop Color-World Test (SCWT) and Boston Naming Test. In the present study, we had considered only participants who underwent the neuropsychological assessment both at the first time point and after 12 months.

### *2.3 MRI Acquisition and Preprocssing*

MRI images were acquired using a 3.0T uMR-890 MRI scanner (United Imaging, Shanghai, China) with a 64-channel coil and simultaneous multislice imaging techniques. The patients were placed in a supine position quietly with their eyes closed but asked to stay awake during the MRI. The MR sequences included high-resolution 3-dimensional T1-weighted imaging and resting-state fMRI. We collected data in Clinical Neuroscience Center, Ruijin Hospital LuWan Branch, Shanghai Jiao Tong University School of Medicine, Shanghai, China.

High-resolution T1-weighted images were acquired as the templates of further functional images for coregistration. The sequences had the following parameters: repetition time (TR) = 7.52 ms, echo time (TE) = 3.4 ms, field of view (FOV) = 256 $\times$ 256 mm, flip angle = 7 degree, thickness = 0.5 mm, no interslice gap, bandwidth = 240 Hz. All of the brain data were acquired in the sagittal plane, yielding 480 continuous slices with an acquired voxel size of 0.5 $\times$ 0.5 $\times$ 0.5 mm$^3$. Eye-closed resting-state imaging was carried out using gradient EPI with the following parameters: TR = 700 ms, TE = 37.2 ms, FOV = 208 $\times$ 208 mm, matrix size = 104 $\times$ 104, resolution = 2.0 $\times$ 2.0 $\times$ 2.0 mm, slice thickness = 2 mm, number of slices = 70, multiple band = 10, flip angle = 52 degree. The acquisition orientation was axial, and the order of acquisition was output for slice timing in the header information as the protocol was simultaneous multi-slice acceleration. A total of 670 whole-brain volumes were acquired.

The rs-fMRI data were preprocessed using the SPM12 software package (v7487, Wellcome Department of Imaging Neuroscience, London, United Kingdom) based on MATLAB 2020a (Mathworks Inc., Sherborn, MA, USA). Briefly, the preprocessing steps consisted of removal of the first ten volumes of resting-state data for magnetization stabilization, field bias correction, slice time correction, and Friston 24-parameter motion correction. Spatial normaliza-

**Table 1. Demographic characteristics, cognitive performance, and APOE genotype of MCI patients.**

| | Stable MCI | | Progressing MCI | | *p* | |
|---|---|---|---|---|---|---|
| Age | 64.88 ± 7.02 | | 69.14 ± 5.64 | | 0.1302 | |
| Sex (M/F) | 36/68 | | 2/12 | | 0.5158 | |
| Education (yr) | 13.13 ± 2.74 | | 11.43 ± 3.31 | | 0.1361 | |
| APOE e4 carrier | 36 | | 8 | | 0.4588 | |
| | Baseline | 12-Month | Baseline | 12-Month | sMCI* | pMCI* |
| MMSE | 28.19 ± 1.25 | 28.33 ± 1.48 | 27.43 ± 2.15 | 25.86 ± 3.29 | 0.499 | 0.249 |
| AVLT immediate | 15.69 ± 4.22 | 18.10 ± 5.26 | 14.29 ± 3.77 | 14.86 ± 4.88 | <0.001 | 0.789 |
| AVLT 5 min | 4.67 ± 2.31 | 5.29 ± 2.91 | 4.43 ± 3.15 | 3.57 ± 3.64 | 0.013 | 0.429 |
| AVLT 20 min | 4.52 ± 2.39 | 5.08 ± 3.09 | 4.00 ± 3.21 | 3.00 ± 3.65 | 0.028 | 0.395 |
| AVLT recognition | 19.94 ± 2.93 | 20.58 ± 3.45 | 19.57 ± 4.35 | 19.43 ± 5.09 | 0.135 | 0.846 |
| CFT copy | 35.10 ± 1.75 | 35.00 ± 2.01 | 30.00 ± 11.50 | 27.43 ± 12.93 | 0.650 | 0.321 |
| CFT recall 30 min | 16.09 ± 8.25 | 18.04 ± 8.13 | 10.14 ± 9.69 | 12.00 ± 9.90 | 0.020 | 0.250 |
| SCWT_Word | 25.24 ± 7.47 | 25.95 ± 6.12 | 30.63 ± 7.82 | 33.03 ± 6.55 | 0.873 | 0.199 |
| SCWT_Color | 43.07 ± 48.27 | 38.69 ± 10.26 | 40.40 ± 8.26 | 48.17 ± 14.28 | 0.404 | 0.022 |
| SCWT_Interfere | 79.17 ± 42.60 | 82.03 ± 37.71 | 84.61 ± 29.51 | 99.56 ± 32.86 | 0.635 | 0.124 |
| TMT_A | 57.55 ± 18.58 | 62.44 ± 22.97 | 85.46 ± 41.51 | 114.33 ± 84.37 | 0.238 | 0.190 |
| TMT_B | 135.27 ± 55.61 | 146.99 ± 62.31 | 212.96 ± 106.23 | 269.44 ± 129.11 | 0.271 | 0.100 |
| BNT | 24.12 ± 3.05 | 23.37 ± 7.55 | 23.86 ± 2.19 | 22.57 ± 6.50 | 0.480 | 0.546 |
| ADAS-Cog | 6.82 ± 3.37 | 5.39 ± 3.53 | 7.94 ± 4.29 | 12.16 ± 5.11 | <0.001 | <0.001 |

M/F, Male/Female; sMCI, Stable mild cognitive impairment; pMCI, Progressed mild cognitive impairment; MMSE, Mini-mental State Examination; AVLT, Auditory Verbal Learning Test; CFT, Complex Figure Test; SCWT, Stroop Color-Word Test; TMT, the Trail Making Test; BNT, Boston naming test; ADAS-Cog, Alzheimer's Disease Assessment Scale–Cognitive Subscale. * Comparison between baseline and 12-month.

tion was performed by Diffeomorphic Anatomical Registration Through Exponentiated Lie algebra (DARTEL) tool for creating a group specific template and for normalizing functional images to the common space [21]. Spatial smoothing was performed in the resultant images using a Gaussian kernel with an 6-mm full-width half-maximum with the modified MATLAB toolbox "Data Processing & Analysis of Brain Imaging (DPABI, version 3.1)" [22]. We excluded patients who had head motion >1.0 mm in any directions. Nuisance covariates, including white matter, cerebrospinal fluid and global signals were further regressed out.

Then a group-level independent component analysis (ICA) was used to define the 25 brain nodes of interest (independent component, IC) as described in previous studies [23,24]. We performed spatial group independent component analysis (ICA) implemented in the Group ICA of functional MRI Toolbox (GIFT v4.0a; http://icatb.sourceforge.net) [25,26]. Resting-state functional MRI data of all patients were firstly decomposed into principal components for subject-specific data reduction, and then spatially decomposed into 25 ICs, each of which exhibited a unique time course profile, based on the Infomax algorithm [27]. The resultant data was converted to Z scores, and ICs with Z score >1.5 can be found in **Supplementary Fig. 1**. We additionally filtered the fMRI data between frequencies of 0.01 and 0.1 Hz.

### *2.4 Sliding-Windows, Multilayer Modularity and Network Switching*

As depicted in Fig. 1, the sliding-window approach was used to explore time-resolved dFNC. Resting-state time-series data were extracted and segmented into a 30-repetition time (TR) window with a size of 21 s, which is convolved with Hamming function to mitigate edge artifacts of the windows and attenuate potentially noisy signals [14]. The window was sliding step-wise by 1 TR along the 660-TR length scan, resulting in a total number of 631 consecutive windows. We chose 30 TRs segmented window length as the grade-off between dynamics of functional connectivity [28] and $1/f0$ wavelength criterion proposed by Zalesky and Breakspear [29]. Here, the pairwise Pearson's correlation coefficient between 25 ICs was calculated in each 21s time window. We thus obtained 631 correlation matrix, and positive matrix values entered the next multilayer network switching analysis. Although some identified clusters might be related to noise, we did not exclude ICs from ICA for the following reasons as in the previous studies [14,30]. In the preprocessing step, nuisance covariates, including white matter, cerebrospinal fluid and global signals were regressed out. Meanwhile, the ICs identified from ICA could not be 100% from noise as they may be in the mid brain (i.e., IC 1). In addition, the switching rate represented the dynamic change of each IC, and it was not greatly influenced by other ICs which might be noise. The elastic net regression analysis automatically selected switching rate of ICs and it could further rule out switching rate of noise.

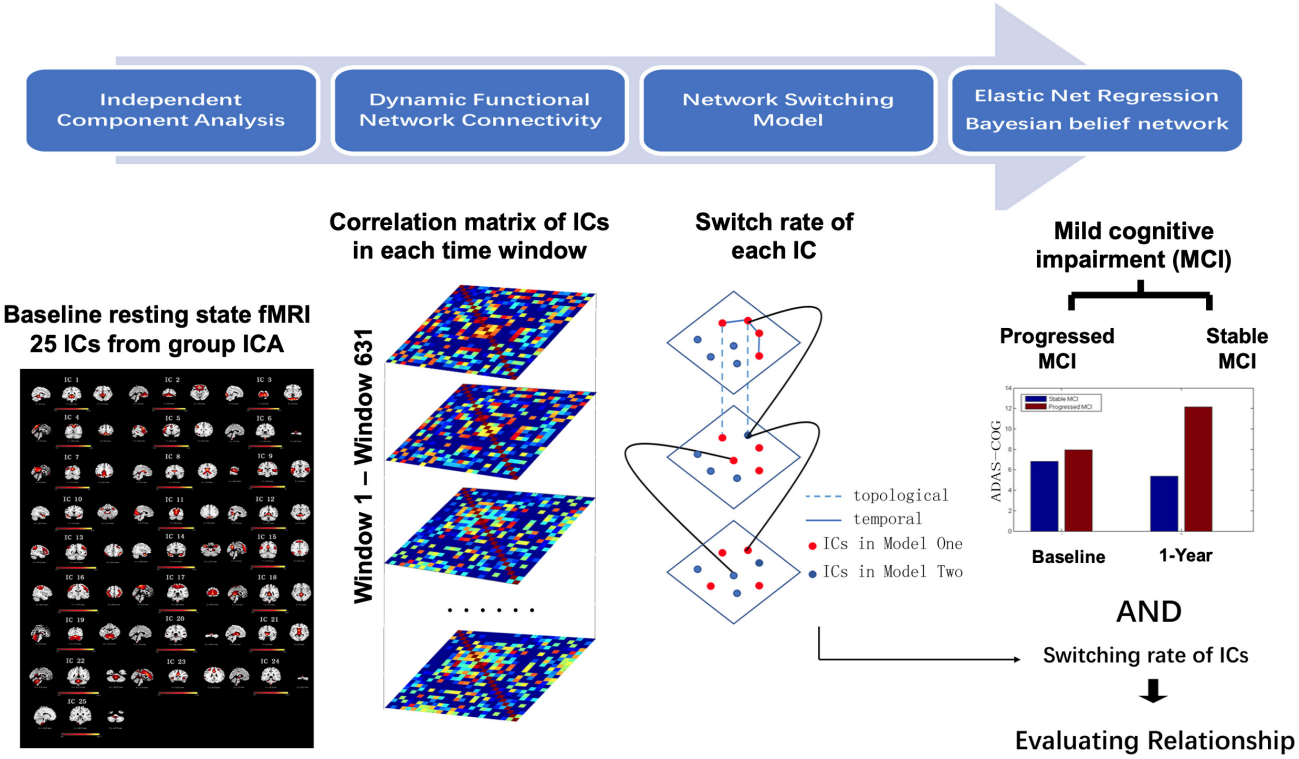


**Fig. 1. Flow diagram shows data processing and patients grouping for the present study.** Abbreviation: MCI, mild cognitive impairment; IC, independent component.

To quantify spatiotemporal network switching, we used an iterative and ordinal Louvain algorithm to track network function over time [31], with the code governing parameters ($\gamma = 1$ and $\omega = 1$) and formula suggested by Pedersen, Zalesky [14]:

$$Q(\gamma,\omega) = \frac{1}{2\mu}\sum_{ijsr}\left[\left(A_{ijs} - \gamma_s \frac{k_{is}k_{js}}{2m_s}\delta\left(M_{is},M_{js}\right) + \delta(i,j)\cdot\omega_{jrs}\right)\right] \delta\left(M_{is},M_{jr}\right)$$

Modularity was quantified by Q ranging from 0 (low network segregation) to 1 (high network segregation). $\delta\left(M_{is},M_{js}\right)$ and $\delta\left(M_{is},M_{jr}\right)$ were 1 if nodes belonged to in the same module and 0 if they did not belong to the same module (M). This process was iterated before the inherent heuristics of the multilayer modularity algorithm converged, which also determined the number of modules per individual. $A_{ijs}$ is the sliding-window correlation matrix between node i and j for time point s. The k was node degree at time point s, and m = sum degree of all nodes at time point s. The $\gamma_s$ is the topological resolution parameter of time point. $\omega_{jrs}$ is the temporal coupling parameter for node j between time window r and s.

Networks had average modularity (Q) of 0.536 $\pm$ 0.026 SD. The final output of the multilayer modularity algorithm was a 25 $\times$ 631 array with integer values denoting modules that each IC was assigned to in the specific time window. The switching rate for each IC was estimated as the percentage of time windows when a brain node transitions between different module assignments.

### *2.5 Elastic Net Regression and Bayesian Belief Network*

We used elastic net regression to test the association between network switching rate of 25 ICs and the individual's cognitive performance at baseline, as well as its changes (12 months - baseline), adjusted for age, sex, and education, and APOE genotype. Elastic net enabled data-driven regression analysis by enforcing sparsity of regression output values and it provided automatic variable selection by removing all ICs not related to cognitive performance. Network switching rates, cognition data were normalized into z-scores to ensure all data were scaled equally. According to previous study, we set the $\alpha$ value to 0.5 to take advantage of the relative strengths of LASSO and Ridge regression approaches, providing a non-sparse solution with low variance among several correlated independent variables [14]. In each regression, we calculated elastic net over a range of different $\lambda$ values between 0 and 1 with increments of 0.001 using 10-fold cross-validation (see equation in the **Supplementary Material**), The selected threshold had lowest mean square error over all possible $\lambda$s across the 10-folds.

Given the $\beta$ from elastic net regression equation in the **Supplementary Material**, we defined prediction as:

$$\text{Prediction } = \mathrm{X}\cdot\beta + \beta_0$$

**Table 2. Parameters of the elastic regression model and switching rate of ICs associated with baseline cognition.**

| | R | *p* | Lambda | MinSE | ICs in the regression model |
|---|---|---|---|---|---|
| MMSE | 0.471 | 0.0002 | 0.1153 | 0.0766 | 1, 3, 5, 13, 19 |
| AVLT immediate | 0.502 | 0.0001 | 0.1011 | 0.0625 | 3, 14 |
| AVLT 5 min | 0.574 | 0.0001 | 0.0931 | 0.0690 | 7, 14, 15 |
| CFT recall 30 min | 0.647 | 0.0001 | 0.0879 | 0.0629 | 10, 12, 17, 21 |
| SCWT_Interfere | 0.444 | 0.0005 | 0.0414 | 0.0211 | 5, 7, 15, 25 |
| TMT_B | 0.498 | 0.0001 | 0.0869 | 0.0374 | 1, 6, 19 |
| BNT | 0.509 | 0.0001 | 0.0898 | 0.0444 | 16, 22 |
| ADAS-word recall | 0.823 | 0.0001 | 0.0236 | 0.0313 | 7, 9, 14, 15, 16 |

IC, independent component; MinSE, minimal mean square error; MMSE, Mini-mental State Examination; AVLT, Auditory Verbal Learning Test; CFT, Complex Figure Test; SCWT, Stroop Color-Word Test; TMT, the Trail Making Test; BNT, Boston naming test; ADAS-Cog, Alzheimer's Disease Assessment Scale–Cognitive Subscale; *p*, significance of regression model.

Where X is the original values of our neuropsychological variables, and $\beta_0$ is the intercept of the elastic net regression model. The significance and Spearman's Rho between prediction and X were calculated for regression evaluation.

In relationship with MMSE, AVLT, STT, CFT, and Boston naming test, positive $\beta$ suggests a positive relationship between switching rate and cognitive performance. On the contrary, positive $\beta$ found in the regression between switching rate and ADAS-Cog or SCWT suggests a negative effect on performance due to the character of the two measurements.

For assessing the association between groups (sMCI and pMCI) and ICs' switching rate, a Bayesian belief network was introduced. Package Bnlearn (version 4.4, Marco Scutari, Lugano, Switzerland) and Caret (version 6.0-81, Max Kuhn, New London, CT, USA) in RStudio software (the R Project for Statistical Computing, R software, version 3.1.0, R Core Team, Boston, MA, USA) was introduced for building a Bayesian belief network and directed acyclic graph. To quantitively define their relationship, we calculated the mean receiver operating characteristic (ROC) curve for the results from the Bayesian belief network. For multiple comparisions, we used Bonferroni correction to minimize the chance of false positive rate.

## 3. Results

### *3.1 Participants*

The age, sex, years of education, and *ApoE* genotype were of no difference between the two groups (Mann-Whitney U-test for continuous data or Chi-square test for categorical data). The pMCI group had significantly declined performance mainly in SCWT and ADAS-Cog test ($p < 0.05$, repeated measures analysis, Table 1). By contrast, sMCI had statistically better cognitive performance in AVLT, CFT and ADAS-Cog after 12-month follow-up. It suggested sMCI of negative trend for cognitive decline. Thus, sMCI could be the control for pMCI patients who would progress to AD with AD clinical and pathological characters.

### *3.2 Independent Components and Correlation with Cognitive Performance*

We identified 25 ICs from baseline resting-state fMRI using the group ICA. Some ICs are topologically consistent with previous results on the networks by visual inspection [24,32]: default mode network (DMN, IC 15), salience network (IC 9), auditory network (IC 10, 14), sensorimotor network (SMN, IC 17), visual network (IC 3, 11), executive control network (ECN, IC 5, 13, 16) and cerebellum network (IC 19, 22). The detailed spatial maps of independent components are listed in **Supplementary Fig. 1**.

The switching rate of each IC was calculated, as shown in **Supplementary Table 1**, and normalized further. The regularization parameter in elastic regression, $\lambda$, and the minimum mean square error was listed in Table 2. With each pair of parameters, the switching rate of several ICs contributed to specific cognitive domains after adjusting the effect from age, sex, education, and *ApoE* genotype. The mapping of IC 15 was comprised of the posterior cingulate and medial prefrontal cortex, suggesting its major role in the DMN. In the models above, a higher switching rate of IC 15 was positively related to global and word recall of ADAS-Cog performance (Table 2).

Besides, the switching rate of the auditory network (IC 14) involved in the AVLT immediate and 5-min recall, and it also positively contributed to ADAS-Cog word recall. DMN (IC 15) also positively contributed to AVLT 5-min recall and ADAS-Cog word recall. The switching rate of SAN (IC 9) and ECN (IC 16) negatively associated with performance in ADAS-Cog word recall. Another component in ECN (IC 5) also negatively associated with MMSE and SCWT-interference (Fig. 2).

### *3.3 Switching Rate Predicted Clinical Progression*

We compared the switching rate of each IC between sMCI and pMCI groups at baseline, and IC 15 had a significantly higher switching rate in the sMCI group (4.1% $\pm$ 1.4% vs. 2.3% $\pm$ 1.5%, $p = 0.0017$). Further, we estimated the predictive effect of switching rates in each ICs

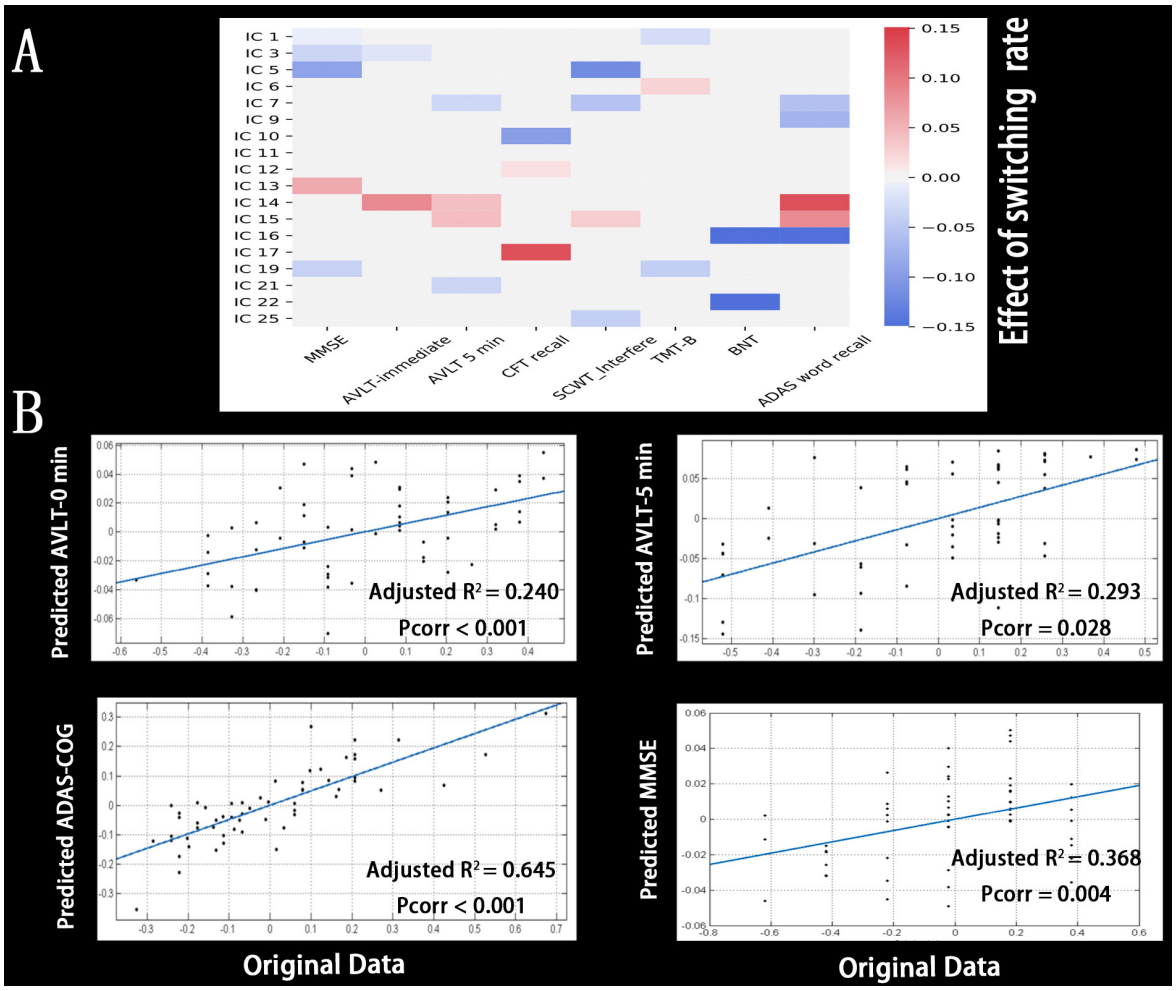


**Fig. 2. Cross-sectional switching rate and cognition.** (A) Contribution of switching rate in each IC to cross-sectional cognitive performance. The positive effect suggested that a higher switching rate correlated with better cognition and vice versa. (B) The fitting between original cognitive performance and predicted data from the elastic regression model, with the input of demographics and switching rate. Abbreviation: IC, independent component; MMSE, Mini-mental State Examination; AVLT, Auditory Verbal Learning Test; CFT, Complex Figure Test; SCWT, Stroop Color-Word Test; TMT, the Trail Making Test; BNT, Boston naming test; ADAS-Cog, Alzheimer's Disease Assessment Scale–Cognitive Subscale.

on the disease progression. In the elastic regression model used above, lower switching rate of IC 15 predicted the MCI progress ($\lambda = 0.169$, mSE = 0.109, r = 0.339, $p = 0.009$) and faster MMSE decline ($\lambda = 0.067$, mSE = 0.038, r = 0.554, $p < 0.001$). By contrast, lower switching rate in SMN (IC 17) contributed to slower cognitive decline in ADAS-Cog, AVLT-5 min and AVLT-20 min recall (Table 3, Fig. 3).

To make the results more consolidated, we used the Bayesian belief network and found that only a lower IC 15 switching rate has an associated effect on the pMCI group (Coefficients of IC 15: –8.135). Since we found the topological association between progress and IC 15, we built a classifier just using IC 15 with a random forest model. The area under the curve was 0.820 ± 0.094.

## 4. Discussion

It has been largely studied that dynamic functional network connectivity serves as a physiological biomarker of cognitive performance. The switching rate of nodes in the network provides novel time-vary connectivity changes in adjacent ICA time windows. Using the data-driven approach of independent component analysis, we observed a set of independently coherent nodes belonging to networks in MCI, which were coincided with functional networks, as previously reported [33]. The relationship between switching rates and behavior has been extensively investigated. In healthy individuals, the whole-brain modularity steadily increased during training for both conditions of the dual n-back task, especially the autonomy of the default mode system. Its integration among task-positive systems was modulated by training [34]. In addition, major depression and bipolar disorder patients decreased network switching

**Table 3. Parameters of the elastic regression model and switching rate of ICs associated with cognition changes.**

| Changes | R | *p* | Lambda | MinSE | ICs in the regression model |
|---|---|---|---|---|---|
| AVLT 5 min | 0.289 | 0.028 | 0.1034 | 0.0300 | 17 |
| AVLT 20 min | 0.554 | 0.001 | 0.0745 | 0.0379 | 1, 10, 17 |
| CFT copy | 0.294 | 0.025 | 0.0605 | 0.0158 | 10, 17 |
| SCWT_Interfere | 0.307 | 0.019 | 0.0757 | 0.0186 | 13 |
| BNT | 0.330 | 0.011 | 0.0842 | 0.0423 | 14, 20, 21 |
| ADAS-Cog | 0.554 | 0.001 | 0.0674 | 0.0376 | 2, 11, 17 |
| sMCI vs pMCI | 0.339 | 0.009 | 0.1691 | 0.1090 | 15 |

No. of IC, Number of independent component; MinSE, minimal mean square error; sMCI, stable mild cognitive impairment; pMCI, progressed mild cognitive impairment; MMSE, Minimental state examination; AVLT, Auditory Verbal Learning Test; CFT, Complex Figure Test; SCWT, Stroop Color-Word Test; TMT, the Trail Making Test; BNT, Boston naming test; ADAS-Cog, Alzheimer's Disease Assessment Scale–Cognitive Subscale; *p*, significance of regression model.

rate of key hubs in default mode network [30]. By contrast, higher 'flexibility' (switching between multilayer network communities) was suggested to be a feature of schizophrenia during working memory task [35]. There was significantly higher flexibility in the thalamus due to default-mode sensory/motor transitions [36]. The present study is the first one to investigate the predictive effect of resting state switching rate in MCI on cross-sectional cognitive performance, as well as MCI conversion to dementia.

In the cross-sectional part, the compelling finding was that, in MCI patients, more frequent switching in the DMN generally suggested better cognition, while the networks related to executive control (ECN) and attention (SAN) had contrary results. It was well-established that the frontal and parietal regions were crucial aspects of the ECN, which sent rich sensory information not only for movement controls, but also for other cognitive abilities, especially in executive function [37]. A meta-analysis study suggested an increase of functional changes in the frontal and parietal regions of MCI [38], which was in line with our results. The attention network was associated with working memory and episodic memory encoding. Recent studies have found intra-network and inter-network functional disruptions in the DAN in MCI patients [39,40]. Mind-body exercise significantly increased the selective attention of MCI patients, and meanwhile decreased functional connectivity in attention network [41].

However, the relationship between the executive control and attention networks with cognition was not found significant longitudinally. The relationship might be obscured by longitudinal u-shaped trajectory in inter-network FC between ECN and DMN [42]. Another possible reason related to neural compensation, which involved frontal regions and the dorsal attention network. Neural compensation was suggested to be common in mild cognitive impairment and Alzheimer's disease [43].

The brain regions of DMN include the precuneus/posterior cingulate cortex (PCC), medial prefrontal cortex (MPFC) and medial, lateral, and inferior parietal cortex [44], which are consistent with our IC 15 mapping. The resting-state DMN changes in aging, MCI, and AD patients have been largely studied, and its activation and inter-network connectivity are generally considered biomarker to dementia [45,46]. The anterior aspect of the DMN was negatively related to cognitive decline in the older group [47]. In the individuals at risk for Alzheimer's disease, APOE $\epsilon$4 carriers demonstrated a slower increase of functional connectivity in frontal lobes within the DMN [48]. Regarding MCI, they demonstrated deactivation of frontal DMN regions, while less significant in Alzheimer's patients [49]. MCI with amyloid deposition showed steeper longitudinal DMN FC declines [50]. In AD patients, a resting-state fMRI study observed reduced functional connectivity between right hippocampus and MPFC, ventral ACC, inferotemporal cortex, right cuneus, right superior, MTG, and PCC [51]. Different from seed-based analysis for functional connectivity, the present study focused on the co-operation of functional networks (e.g., DMN, ECN, SAN). Based on the networks derived from ICA, seed-based analysis only explored the strength of inter- or extra-network connectivity. However, we used dynamic strength changes between networks during the acquisition time span to calculate the modularity of networks. For instance, in one state, DMN and ECN had strong connection and they belonged to the same module. In the next state, DMN switched to another module and might have strong connection with SAN. The transition represented segregation of DMN and ECN, as well as integration of DMN and SAN. As described in the Method section, the switching rate for each network was estimated as the percentage of network transitions across different modules.

We further focused on the switching rate of DMN and its relationship with MCI cognition. The resting brain's functional organization was suggested to be configured to maintain a balance between network segregation and inte-

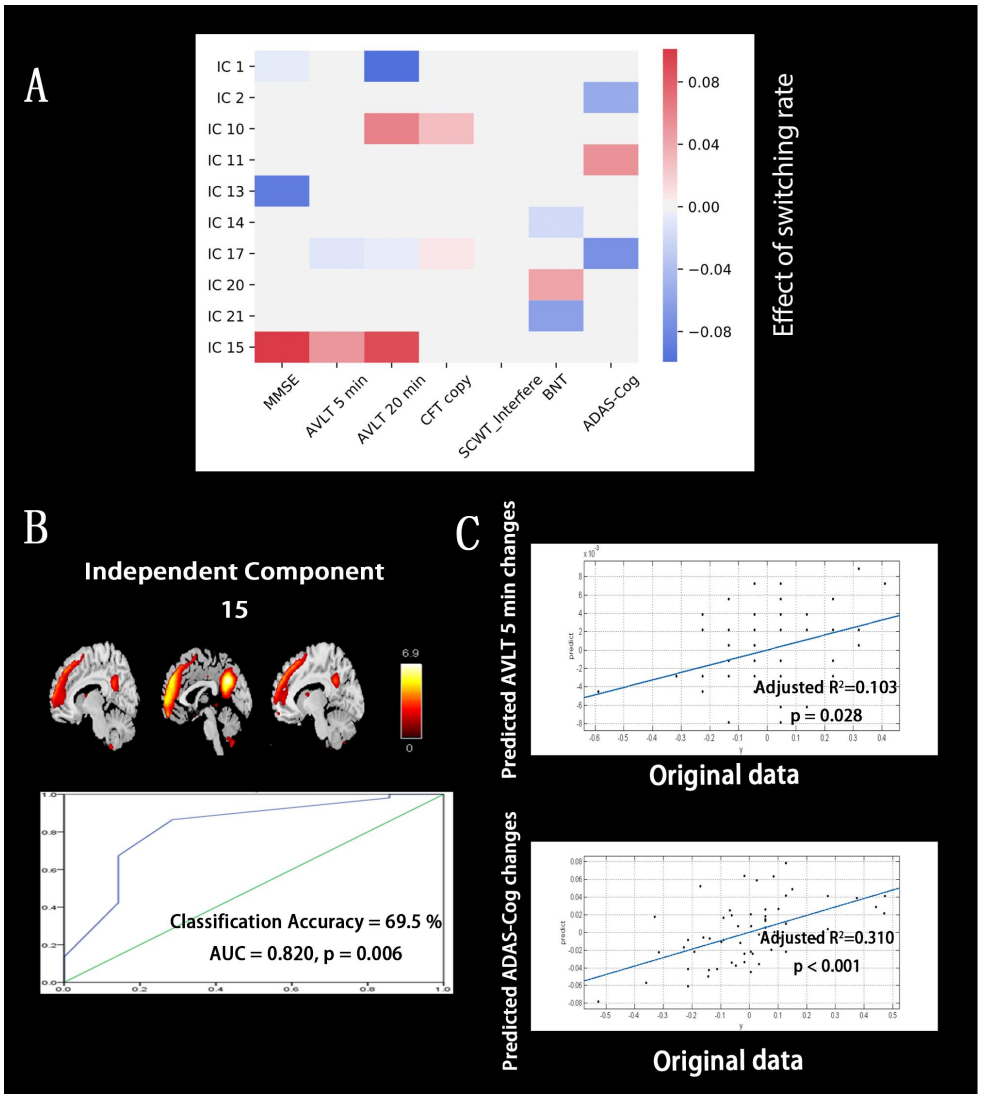


**Fig. 3. Switching rate and longitudinal cognition changes.** (A) Contribution of switching rate in each IC to longitudinal cognitive changes. The positive effect suggested that a higher switching rate correlated with better cognition endpoints. (B) The mapping of IC 15 and the ROC curve for MCI grouping by IC 15's switching rate. (C) The fitting between original cognitive performance changes and predicted changes from the elastic regression model. Abbreviation: IC, independent component; MMSE, Mini-mental State Examination; AVLT, Auditory Verbal Learning Test; CFT, Complex Figure Test; SCWT, Stroop Color-Word Test; TMT, the Trail Making Test; BNT, Boston naming test; ADAS-Cog, Alzheimer's Disease Assessment Scale–Cognitive Subscale.

gration. This functional balance was associated with better memory. Furthermore, brain tending toward stronger segregation versus integration foster different cognitive abilities [52]. Thus, our results suggested DMN switching rate as marker for cognitive abilities in MCI and AD.

Amyloid and tau burden also showed their association with DMN. DMN functional connectivity during rest is altered with increasing amyloid-PET signal levels in aging and AD patients [53,54]. In the early phase of AD, hyperconnectivity in the DMN was associated with neocortical tau in the positive amyloid individuals, while hypoconnectivity was observed when tau level elevated [55]. As switching of DMN is presumed to be related to increased information load on the related brain regions [56], our observations closely resemble the trend of DMN changes in MCI and AD. This reduction in DMN switching rate was closely linked to the clinical severity of MCI patients, especially the short-term memory and executive function by data-driven elastic net regression. The difference in IC 15 switching rate between groups was consolidated by elastic net regression for grouping and Bayesian belief network validation.

While the DMN is generally regarded as active when the brain is at wakeful rest, it is negatively correlated with other networks [57]. We also observed inverse switching rate changes in some other resting-state networks. Worse memory and executive function in MCI correlated with increased switching rate in ECN and SAN. It implies the

higher entropy or information load on the specific brain regions illustrated in IC 5, 9, 13, and 16 [58], especially on the bilateral inferior parietal cortex. The association cortex was known to integrate information between a range of different networks, and might act as compensation [59]. The observed increased switching rate in ECN showed some resemblance to the functional connectivity changes in ECN of MCI and AD patients. The mild AD showed significantly increased resting-state functional in ECN compared to healthy controls, as well as increased rsFC in ECN compared to MCI [60]. In the effective connectivity study for MCI and AD, in contrary to connectivity from the DMN to the other resting-state networks, increased connectivity was evident between the memory network and the ECN in the AD and MCI patients [61].

Longitudinal data in the present study also demonstrated the ominous effects of the higher switching rate of SMN. Several studies of Alzheimer's disease have also identified changed functional connectivity in the sensorimotor network indicative of compensation or covert biomarker [62,63]. Amnesic MCI showed increased FC between the supplementary motor area with the superior parietal lobe in the SMN, while the DMN has reduced internetwork connectivity with the SMN [64]. Although statistical association was found between cognitive tests (i.e., AVLT, ADAS-Cog and CFT-copy) and switching rate of IC 17 in SMN, the association was not strong to further show the relationship between SMN and MCI/AD conversion. The potential compensation role of SMN in MCI stages need to be further studied.

It is suggested that the motor cortex is involved in the initial stages of AD, and its hyperexcitability is a well-defined neurophysiological feature of early AD [54,65,66]. The increased ability of excitation was regarded as its ability to plastically reorganize itself via recruiting extra cortical circuits in the SMN, or other alternative circuits [66], due to its natural distributed network with multiple representations of the motor maps [67]. The motor cortex hyperexcitability would be due to an imbalance between excitatory and inhibitory circuits, probably induced by $\beta$ amyloid deposition [66,68], glutamatergic over-activation, and reduction of GABA mediated inhibition [69]. The phenomenon has great clinical sense as the parameter is related to disease severity and progression, and could be intervened by transcranial magnetic stimulation [68,70].

There are a few limitations that should be considered in the interpretation of our results. First, the parameter of temporal resolution and length of acquisition in BOLD signal sampling should be carefully checked for reliable results. Previous studies suggested much higher temporal resolution [14,71] and longer resting-state session (57.6 min), which could merely be possible in clinical practice. Though temporal down-sampling of fMRI networks has similar results in the previous study [14], it is necessary to re-test the multilayer network modularity detection in a larger sample of MCI for further validation. Second, the length of the time window was discussed and varied in different studies [28,33]. The reliability caused by different time window needs to be optimized by more accurate computational methods. Finally, due to the moderate sample size (118 MCI) and relatively short follow-up period for patients (1 year), the MCI conversion rate is low (14 in 118) and posed difficulty in constructing the predictive model. Further studies with larger sample size and longer follow-up periods would allow for the examination of MCI conversion.

## 5. Conclusions

In summary, the switching rate of resting-state networks serves as a novel biomarker for cognitive performance in MCI patients, as well as a predictive marker for disease progression. Among them, DMN switches as a representation of slow cognitive decline, while switching of SMN heralds worsening. The biomarker-guided predictive models will further permit researchers to identify and stratify MCI populations.

## Author Contributions

ZH and BL designed the research study. ZH and YD performed the research. BL analyzed the data. ZH and BL wrote the manuscript. All authors contributed to editorial changes in the manuscript. All authors read and approved the final manuscript.

## Ethics Approval and Consent to Participate

All subjects gave their informed consent for inclusion before they participated in the study. The study was conducted in accordance with the Declaration of Helsinki, and the protocol was approved by the Ethics Committee of Ruijin Hospital, Shanghai Jiao Tong University School of Medicine (No. 2021-337).

## Acknowledgment

We thank all the researchers in the SIMPLE study. We acknowledge the altruism of SIMPLE participants and their families.

## Funding

This work was supported by Shanghai Rising-Star Program (21QA1405800).

## Conflict of Interest

The authors declare no conflict of interest.

## Supplementary Material

Supplementary material associated with this article can be found, in the online version, at https://doi.org/10.31083/j.jin2106170.

## References

[1] Lin Y, Li B, Tang H, Xu Q, Wu Y, Cheng Q, *et al*. Shanghai cognitive intervention of mild cognitive impairment for delaying progress with longitudinal evaluation-a prospective, randomized

controlled study (SIMPLE): rationale, design, and methodology. BMC Neurology. 2018; 18: 103.
[2] Grundman M. Mild Cognitive Impairment can be Distinguished from Alzheimer Disease and Normal Aging for Clinical Trials. Archives of Neurology. 2004; 61: 59–66.
[3] van Maurik IS, Vos SJ, Bos I, Bouwman FH, Teunissen CE, Scheltens P, *et al*. Biomarker-based prognosis for people with mild cognitive impairment (ABIDE): a modelling study. The Lancet Neurology. 2019; 18: 1034–1044.
[4] Varatharajah Y, Ramanan VK, Iyer R, Vemuri P. Predicting Short-term MCI-to-AD Progression Using Imaging, CSF, Genetic Factors, Cognitive Resilience, and Demographics. Scientific Reports. 2019; 9: 2235.
[5] Du X, Wang X, Geng M. Alzheimer's disease hypothesis and related therapies. Translational Neurodegeneration. 2018; 7: 2.
[6] Gauthier S, Zhang H, Ng KP, Pascoal TA, Rosa-Neto P. Impact of the biological definition of Alzheimer's disease using amyloid, tau and neurodegeneration (ATN): what about the role of vascular changes, inflammation, Lewy body pathology? Translational Neurodegeneration. 2018; 7: 12.
[7] Bassett DS, Wymbs NF, Porter MA, Mucha PJ, Carlson JM, Grafton ST. Dynamic reconfiguration of human brain networks during learning. Proceedings of the National Academy of Sciences. 2011; 108: 7641–7646.
[8] Hutchison RM, Womelsdorf T, Allen EA, Bandettini PA, Calhoun VD, Corbetta M, *et al*. Dynamic functional connectivity: Promise, issues, and interpretations. NeuroImage. 2013; 80: 360–378.
[9] De Domenico M. Multilayer modeling and analysis of human brain networks. GigaScience. 2017; 6: 1–8
[10] Bassett DS, Porter MA, Wymbs NF, Grafton ST, Carlson JM, Mucha PJ. Robust detection of dynamic community structure in networks. Chaos. 2013; 23: 013142.
[11] Shine JM, Koyejo O, Poldrack RA. Temporal metastates are associated with differential patterns of time-resolved connectivity, network topology, and attention. Proceedings of the National Academy of Sciences. 2016; 113: 9888–9891.
[12] Braun U, Schäfer A, Walter H, Erk S, Romanczuk-Seiferth N, Haddad L, *et al*. Dynamic reconfiguration of frontal brain networks during executive cognition in humans. Proceedings of the National Academy of Sciences. 2015; 112: 11678–11683.
[13] Telesford QK, Ashourvan A, Wymbs NF, Grafton ST, Vettel JM, Bassett DS. Cohesive network reconfiguration accompanies extended training. Human Brain Mapping. 2017; 38: 4744–4759.
[14] Pedersen M, Zalesky A, Omidvarnia A, Jackson GD. Multilayer network switching rate predicts brain performance. Proceedings of the National Academy of Sciences. 2018; 115: 13376–13381.
[15] McKhann GM, Knopman DS, Chertkow H, Hyman BT, Jack CR Jr, Kawas CH, *et al*. The diagnosis of dementia due to Alzheimer's disease: recommendations from the National Institute on Aging-Alzheimer's Association workgroups on diagnostic guidelines for Alzheimer's disease. Alzheimer's & Dementia. 2011; 7: 263–269.
[16] Pascoal TA, Mathotaarachchi S, Shin M, Park AY, Mohades S, Benedet AL, *et al*. Amyloid and tau signatures of brain metabolic decline in preclinical Alzheimer's disease. European Journal of Nuclear Medicine and Molecular Imaging. 2018; 45: 1021–1030.
[17] Zhang Z, Hong Z, Wang Y, He L, Wang N, Zhao Z, *et al*. Rivastigmine Patch in Chinese Patients with Probable Alzheimer's disease: a 24-week, Randomized, Double-Blind Parallel-Group Study Comparing Rivastigmine Patch (9.5 mg/24 h) with Capsule (6 mg Twice Daily) CNS Neuroscience & Therapeutics. 2016; 22: 488–496.
[18] Zhao Q, Lv Y, Zhou Y, Hong Z, Guo Q. Short-term delayed recall of auditory verbal learning test is equivalent to long-term delayed recall for identifying amnestic mild cognitive impairment. PLoS ONE. 2012; 7: e51157.
[19] Zhao Q, Guo Q, Li F, Zhou Y, Wang B, Hong Z. The Shape Trail Test: application of a new variant of the Trail making test. PLoS ONE. 2013; 8: e57333.
[20] Zhao Q, Guo Q, Liang X, Chen M, Zhou Y, Ding D, *et al*. Auditory Verbal Learning Test is Superior to Rey-Osterrieth Complex Figure Memory for Predicting Mild Cognitive Impairment to Alzheimer's Disease. Current Alzheimer Research. 2015; 12: 520–526.
[21] Klein A, Andersson J, Ardekani BA, Ashburner J, Avants B, Chiang M, *et al*. Evaluation of 14 nonlinear deformation algorithms applied to human brain MRI registration. NeuroImage. 2009; 46: 786–802.
[22] Yan CG, Wang XD, Zuo XN, Zang YF. DPABI: Data Processing & Analysis for (Resting-State) Brain Imaging. Neuroinformatics. 2016; 14: 339–351.
[23] Fiorenzato E, Strafella AP, Kim J, Schifano R, Weis L, Antonini A, *et al*. Dynamic functional connectivity changes associated with dementia in Parkinson's disease. Brain. 2019; 142: 2860–2872.
[24] Kim J, Criaud M, Cho SS, Díez-Cirarda M, Mihaescu A, Coakeley S, *et al*. Abnormal intrinsic brain functional network dynamics in Parkinson's disease. Brain. 2017; 140: 2955–2967.
[25] Calhoun VD, Adali T, Pearlson GD, Pekar JJ. A method for making group inferences from functional MRI data using independent component analysis. Human Brain Mapping. 2001; 14: 140–151.
[26] Erhardt EB, Rachakonda S, Bedrick EJ, Allen EA, Adali T, Calhoun VD. Comparison of multi-subject ICA methods for analysis of fMRI data. Human Brain Mapping. 2011; 32: 2075–2095.
[27] Bell AJ, Sejnowski TJ. An Information-Maximization Approach to Blind Separation and Blind Deconvolution. Neural Computation. 1995; 7: 1129–1159.
[28] Allen EA, Damaraju E, Plis SM, Erhardt EB, Eichele T, Calhoun VD. Tracking whole-Brain Connectivity Dynamics in the Resting State. Cerebral Cortex. 2014; 24: 663–676.
[29] Zalesky A, Breakspear M. Towards a statistical test for functional connectivity dynamics. NeuroImage. 2015; 114: 466–470.
[30] Han S, Cui Q, Wang X, Li L, Li D, He Z, *et al*. Resting state functional network switching rate is differently altered in bipolar disorder and major depressive disorder. Human Brain Mapping. 2020; 41: 3295–3304.
[31] Mucha PJ, Richardson T, Macon K, Porter MA, Onnela J. Community Structure in Time-Dependent, Multiscale, and Multiplex Networks. Science. 2010; 328: 876–878.
[32] Beckmann CF, DeLuca M, Devlin JT, Smith SM. Investigations into resting-state connectivity using independent component analysis. Philosophical Transactions of the Royal Society B: Biological Sciences. 2005; 360: 1001–1013.
[33] Shirer WR, Ryali S, Rykhlevskaia E, Menon V, Greicius MD. Decoding Subject-Driven Cognitive States with whole-Brain Connectivity Patterns. Cerebral Cortex. 2012; 22: 158–165.
[34] Finc K, Bonna K, He X, Lydon-Staley DM, Kühn S, Duch W, *et al*. Dynamic reconfiguration of functional brain networks during working memory training. Nature Communications. 2020; 11: 2435.
[35] Braun U, Schäfer A, Bassett DS, Rausch F, Schweiger JI, Bilek E, *et al*. Dynamic brain network reconfiguration as a potential schizophrenia genetic risk mechanism modulated by NMDA receptor function. Proceedings of the National Academy of Sciences. 2016; 113: 12568–12573.
[36] Gifford G, Crossley N, Kempton MJ, Morgan S, Dazzan P, Young J, *et al*. Resting state fMRI based multilayer network configuration in patients with schizophrenia. NeuroImage: Clinical. 2020; 25: 102169.
[37] Roh HW, Choi J, Kim N, Choe YS, Choi JW, Cho S, *et al*. Associations of rest-activity patterns with amyloid bur-

den, medial temporal lobe atrophy, and cognitive impairment. EBioMedicine. 2020; 58: 102881.
[38] Xu W, Chen S, Xue C, Hu G, Ma W, Qi W, *et al*. Functional MRI-Specific Alterations in Executive Control Network in Mild Cognitive Impairment: An ALE Meta-Analysis. Frontiers in Aging Neuroscience. 2020; 12: 578863.
[39] Wu H, Song Y, Chen S, Ge H, Yan Z, Qi W, *et al*. An Activation Likelihood Estimation Meta-Analysis of Specific Functional Alterations in Dorsal Attention Network in Mild Cognitive Impairment. Frontiers in Neuroscience. 2022; 16: 876568.
[40] Bi XA, Sun Q, Zhao J, Xu Q, Wang L. Non-linear ICA Analysis of Resting-State fMRI in Mild Cognitive Impairment. Frontiers in Neuroscience. 2018; 12: 413.
[41] Xia R, Qiu P, Lin H, Ye B, Wan M, Li M, *et al*. The Effect of Traditional Chinese Mind-Body Exercise (Baduanjin) and Brisk Walking on the Dorsal Attention Network in Older Adults With Mild Cognitive Impairment. Frontiers in Psychology. 2019; 10: 2075.
[42] Ng KK, Lo JC, Lim JKW, Chee MWL, Zhou J. Reduced functional segregation between the default mode network and the executive control network in healthy older adults: a longitudinal study. NeuroImage. 2016; 133: 321–330.
[43] Anthony M, Lin F. A Systematic Review for Functional Neuroimaging Studies of Cognitive Reserve across the Cognitive Aging Spectrum. Archives of Clinical Neuropsychology. 2018; 33: 937–948.
[44] Raichle ME, MacLeod AM, Snyder AZ, Powers WJ, Gusnard DA, Shulman GL. A default mode of brain function. Proceedings of the National Academy of Sciences. 2001; 98: 676–682.
[45] Greicius MD, Srivastava G, Reiss AL, Menon V. Default-mode network activity distinguishes Alzheimer's disease from healthy aging: Evidence from functional MRI. Proceedings of the National Academy of Sciences. 2004; 101: 4637–4642.
[46] Koch W, Teipel S, Mueller S, Benninghoff J, Wagner M, Bokde ALW, *et al*. Diagnostic power of default mode network resting state fMRI in the detection of Alzheimer's disease. Neurobiology of Aging. 2012; 33: 466–478.
[47] Damoiseaux JS, Beckmann CF, Arigita EJS, Barkhof F, Scheltens P, Stam CJ, *et al*. Reduced resting-state brain activity in the "default network" in normal aging. Cerebral Cortex. 2008; 18: 1856–1864.
[48] Chiesa PA, Cavedo E, Vergallo A, Lista S, Potier M, Habert M, *et al*. Differential default mode network trajectories in asymptomatic individuals at risk for Alzheimer's disease. Alzheimer'S & Dementia. 2019; 15: 940–950.
[49] Rombouts SARB, Barkhof F, Goekoop R, Stam CJ, Scheltens P. Altered resting state networks in mild cognitive impairment and mild Alzheimer's disease: an fMRI study. Human Brain Mapping. 2005; 26: 231–239.
[50] Chong JSX, Jang H, Kim HJ, Ng KK, Na DL, Lee JH, *et al*. Amyloid and cerebrovascular burden divergently influence brain functional network changes over time. Neurology. 2019; 93: e1514–e1525.
[51] Wang L, Zang Y, He Y, Liang M, Zhang X, Tian L, *et al*. Changes in hippocampal connectivity in the early stages of Alzheimer's disease: Evidence from resting state fMRI. NeuroImage. 2006; 31: 496–504.
[52] Wang R, Liu M, Cheng X, Wu Y, Hildebrandt A, Zhou C. Segregation, integration, and balance of large-scale resting brain networks configure different cognitive abilities. Proceedings of the National Academy of Sciences. 2021; 118: e2022288118.
[53] Mormino EC, Smiljic A, Hayenga AO, H. Onami S, Greicius MD, Rabinovici GD, *et al*. Relationships between Beta-Amyloid and Functional Connectivity in Different Components of the Default Mode Network in Aging. Cerebral Cortex. 2011; 21: 2399–2407.
[54] Sheline YI, Raichle ME, Snyder AZ, Morris JC, Head D, Wang S, *et al*. Amyloid Plaques Disrupt Resting State Default Mode Network Connectivity in Cognitively Normal Elderly. Biological Psychiatry. 2010; 67: 584–587.
[55] Schultz AP, Chhatwal JP, Hedden T, Mormino EC, Hanseeuw BJ, Sepulcre J, *et al*. Phases of Hyperconnectivity and Hypoconnectivity in the Default Mode and Salience Networks Track with Amyloid and Tau in Clinically Normal Individuals. The Journal of Neuroscience. 2017; 37: 4323–4331.
[56] Amigó JM, Kloeden PE, Giménez Á. Entropy Increase in Switching Systems. Entropy. 2013; 15: 2363–2383.
[57] Broyd SJ, Demanuele C, Debener S, Helps SK, James CJ, Sonuga-Barke EJS. Default-mode brain dysfunction in mental disorders: a systematic review. Neuroscience & Biobehavioral Reviews. 2009; 33: 279–296.
[58] Richman JS, Moorman JR. Physiological time-series analysis using approximate entropy and sample entropy. American Journal of Physiology-Heart and Circulatory Physiology. 2000; 278: H2039–H2049.
[59] van den Heuvel MP, Sporns O. Rich-Club Organization of the Human Connectome. Journal of Neuroscience. 2011; 31: 15775–15786.
[60] Joshi H, Bharath S, Balachandar R, Sadanand S, Vishwakarma HV, Aiyappan S, *et al*. Differentiation of Early Alzheimer's Disease, Mild Cognitive Impairment, and Cognitively Healthy Elderly Samples Using Multimodal Neuroimaging Indices. Brain Connectivity. 2019; 9: 730–741.
[61] Chen Y, Yan H, Han Z, Bi Y, Chen H, Liu J, *et al*. Functional Activity and Connectivity Differences of Five Resting-State Networks in Patients with Alzheimer's Disease or Mild Cognitive Impairment. Current Alzheimer Research. 2016; 13: 234–242.
[62] Prieto del Val L, Cantero JL, Baena D, Atienza M. Damage of the temporal lobe and APOE status determine neural compensation in mild cognitive impairment. Cortex. 2018; 101: 136–153.
[63] Babiloni C, Babiloni F, Carducci F, Cincotti F, Del Percio C, De Pino G, *et al*. Movement-Related Electroencephalographic Reactivity in Alzheimer Disease. NeuroImage. 2000; 12: 139–146.
[64] Cai S, Chong T, Peng Y, Shen W, Li J, von Deneen KM, *et al*. Altered functional brain networks in amnestic mild cognitive impairment: a resting-state fMRI study. Brain Imaging and Behavior. 2017; 11: 619–631.
[65] Di Lazzaro V, Oliviero A, Tonali PA, Marra C, Daniele A, Profice P, *et al*. Noninvasive in vivo assessment of cholinergic cortical circuits in AD using transcranial magnetic stimulation. Neurology. 2002; 59: 392–397.
[66] Ferreri F, Pauri F, Pasqualetti P, Fini R, Dal Forno G, Rossini PM. Motor cortex excitability in Alzheimer's disease: a transcranial magnetic stimulation study. Annals of Neurology. 2003; 53: 102–108.
[67] Sanes JN, Donoghue JP. Plasticity and Primary Motor Cortex. Annual Review of Neuroscience. 2000; 23: 393–415.
[68] Ferreri F, Pasqualetti P, Määttä S, Ponzo D, Guerra A, Bressi F, *et al*. Motor cortex excitability in Alzheimer's disease: a transcranial magnetic stimulation follow-up study. Neuroscience Letters. 2011; 492: 94–98.
[69] Paula-Lima AC, Brito-Moreira J, Ferreira ST. Deregulation of excitatory neurotransmission underlying synapse failure in Alzheimer's disease. Journal of Neurochemistry. 2013; 126: 191–202.
[70] Khedr EM, Ahmed MA, Darwish ES, Ali AM. The relationship between motor cortex excitability and severity of Alzheimer's disease: a transcranial magnetic stimulation study. Neurophysiologie Clinique/Clinical Neurophysiology. 2011; 41: 107–113.
[71] Hindriks R, Adhikari MH, Murayama Y, Ganzetti M, Mantini D, Logothetis NK, Deco G. Can sliding-window correlations reveal dynamic functional connectivity in resting-state fMRI? NeuroImage. 2016; 127: 242–256.